RSC Advances

PAPER

View Article Online
View Journal | View Issue

Cite this: *RSC Adv.*, 2018, **8**, 35521

The further activation and functionalization of semicoke for CO_2 capture from flue gases†

Xia Wang, *[a] Wulan Zeng,[a] Qingjie Guo,[b] Qijin Geng,[a] Yongmei Yan[a] and Xiude Hu[b]

Received 11th September 2018
Accepted 11th October 2018

DOI: 10.1039/c8ra07560c

rsc.li/rsc-advances

To systematically study CO_2 adsorption performance, semicoke from the low-rank lignite was further activated and functionalized for CO_2 capture from flue gases. The effect of the activation conditions, such as the activation temperature, activation time and HCl washing, and the tetraethylenepentamine (TEPA)-functionalization on CO_2 adsorption were investigated; the pore structure and surface morphology of the semicoke under different activation conditions were characterized. Both the surface structure and adsorption performance of the activated semicoke could be improved under appropriate activation and acid-treatment conditions. The optimal breakthrough and equilibrium adsorption capacity for the TEPA-functionalized HCl-washed activated semicoke were separately 2.68 and 3.70 mmol g^{-1} at 60 °C for the simulated flue gas of 15 vol% CO_2 and 85 vol% N_2. After ten adsorption–desorption cycles, the equilibrium adsorption capacity was still 3.43 mmol g^{-1}, and the semicoke-based sorbent showed good regenerability.

1. Introduction

In the fifth assessment report of the Intergovernmental Panel on Climate Change (IPCC), CO_2 has been confirmed as the main greenhouse gas and has the greatest contribution to the greenhouse effect.[1] CO_2 capture and storage from large stationary sources such as power plants have received great concern. Around the world, fossil fuels are still the main sources of energy,[2] and in China, the combustion of coal accounts for approximately two-thirds of the total energy source, making a great contribution to environmental deterioration. Therefore, effective strategies are required to fulfill effective CO_2 capture from flue gases in coal-fired power plants around the world.

Currently, the solid sorbents are considered to be more effective and low-corrosion,[3] which can be classified as physical adsorbents and chemical adsorbents according to the adsorption mechanism. The active carbons (ACs) with high surface area and large micropore volume are economical physisorbents, which showed good CO_2 adsorption performance at low temperature.[4] The amine-functionalized porous supporting materials, as potential chemisorbents, are widely studied and approved. Both the aminosilane-grafted and TEPA/polyethylenimine (PEI)-impregnated sorbents showed good CO_2 adsorption performance and regenerability, such as amine-functionalized mesoporous molecular sieves (MCM-41, SBA-15, SAPO-34, *etc.*),[5–8] amine-loaded mesoporous silica,[9–14] amine-immobilized silica nanotubes and nanowires,[15,16] amine-functionalized periodic mesoporous benzenesilicas,[17] amine-functionalized poly (ionic liquid) brushes,[18] amine-grafted metal–organic framework (ZMOF),[19] amine-functionalized porous silicas,[20,21] and amine-functionalized periodic mesoporous phenylene-silicas,[22,23] *etc.* However, the complex preparation process and expensive price for preparing above-mentioned porous supporting materials may limit the large-scale application. Hence, the development of the porous supporting materials with low cost and abundant supply are essential to the long-term application. Wang *et al.* used the low cost and naturally abundant clay as the raw material to develop the porous supporting material by acid or alkaline-treatment, and prepared the PEI-modified composite sorbent.[24] The PEI-modified HCl-treated clay showed good adsorption capacity of 2.55 mmol g^{-1} at 75 °C under dry conditions, and good regenerability after ten adsorption–desorption cycles. Stevens *et al.* prepared the diamine-grafted montmorillonite *via* water aided exfoliation/grafting method, and the prepared sorbent showed good CO_2 selectivity, adsorption capacity and regenerability, and the adsorption capacity reached 1.8 mmol g^{-1} in a 15% CO_2 in N_2 mixture and 2.4 mmol g^{-1} in pure CO_2.[25] Sarmah *et al.* prepared the mixed primary/tertiary amines (MEA/DMA) and mixed secondary/tertiary amines (MEA/DMA)-impregnated fly ash-based sorbents, and the equilibrium adsorption capacity was up to 6.89 and 5.99 mmol g^{-1} in pure CO_2, respectively.[26]

The world's coal reserves are very rich, ranking first among all energy sources, and pores and cracks formed in the process of preparing semicoke. Many researchers have studied the CO_2

[a]*Department of Chemistry and Chemical Engineering, Weifang University, Weifang 261061, Shandong, China. E-mail: xiawangwfu@163.com; Fax: +86 536 8785283; Tel: +86 536 8785283*

[b]*State Key Laboratory of High-efficiency Utilization of Coal and Green Chemical Engineering, Ningxia University, Yinchuan 750021, China*

† Electronic supplementary information (ESI) available. See DOI: 10.1039/c8ra07560c

adsorption performance of the coal and semicoke.[27–30] Comparing with coal, semicoke showed better adsorption performance due to the relatively developed pore and fissure structures and abundant surface functional groups.[31] To further improve the pore structure of the semicoke, in our previous study, semicoke was first activated for 2 h in N_2 at the temperature of 700 °C, and the activated semicoke before and after TEPA-functionalization showed good CO_2 adsorption performance.[32] However, in the early stage, the activation factors that may influence the pore structure development and surface functional groups building for semicoke were not systematically studied due to the limited conditions.

In this research, the effects of the activation temperature, activation time, acid-treating and TEPA-functionalization on CO_2 adsorption of the semicoke were further systematically investigated, the pore structure and surface morphology of the semicoke were characterized, and the regenerability of the TEPA-functionalized semicoke-based sorbent was also studied.

2. Experimental section

2.1. Materials

Ordos coal was provided by Ordos Coal Authority, Nei Monggol, China. The TEPA and HCl were purchased from Shanghai Aladdin Bio-Chem. Technology Co., Ltd, Shanghai, China. Anhydrous ethanol (AR) was bought from Beijing Chem. Factory, Beijing, China. Highly pure N_2 and simulated flue gas with a volume ratio of 15% CO_2 to 85% N_2 were distributed in Qingdao Heli Gas Co., Ltd., Qingdao, China.

2.2. The activation and acid-reating of semicoke

According to the previous study, the low-rank lignite of Ordos coal with non-coking property was selected to prepare the semicoke.[28,33] The coal was ground to powder and further sifted to the particle size of below 0.15 mm, and then transferred into the drying oven to eliminate the adsorbed water. The dried powder was placed in the self-assembled fixed-bed reactor and passed in N_2 for 30 min to replace the air and moisture in the reactor, at this time the system was heated up to 500 °C at the rate of 20 K min^{-1} and maintained at 500 °C for 1 h, then the system was cooled to the room temperature in N_2. The semicoke formed and was marked as SE for short, which was further treated to prepare the activated semicoke.[7,34] The semicoke loaded in the reactor was heated up to a set temperature under N_2 atmosphere for a certain time, then the system was cooled to the room temperature, and the activated semicoke formed, which was designated as SEa-b for short, with *a* and *b* representing the activation temperature (°C) and activation time (h), respectively.

A certain weight of the activated semicoke was added to the uniformly stirring HCl of 6 mol L^{-1} for 2 h, then the powder was filtered and washed with distilled water until the pH was approximate 7. The dried powder was designated as SEa-b(6) for short, with 6 representing the molar concentration of HCl.

The amine-functionalization of the activated semicoke before and after HCl treating used the impregnation method.[35] Considering the development content of the pore structure, the weight loading percentage for TEPA was set to 10%. 0.11 mL of TEPA was dissolved in 20 mL of anhydrous ethanol and sonicated for 30 min, then 1 g of the activated semicoke was quickly added to the solution and the suspension was continuously sonicated for 3 h, which was then transferred into the vacuum drying oven at 85 °C for 24 h. The dried powder was abbreviated as SEa-b-TEPA10% or SEa-b(6)-TEPA10%, with 10% being the weight loading percentage of TEPA.

2.3. CO_2 adsorption and regeneration experiments

The CO_2 adsorption and regeneration experiments were performed in a fixed-bed reactor,[5] which is a quartz tube with the inner diameter of 0.8 mm and length of 40 mm. 0.9 g of the dried sample was put in the reactor and N_2 was passed through to expel the air, then the reactor was heated to 100 °C and kept at this temperature for 1 h to desorb the adsorbed air and moisture. Then the temperature was decreased to a set temperature and N_2 was simultaneously transferred to the simulated flue gas with the influent velocity of 30 mL min^{-1}, and the CO_2 adsorption stage began. The CO_2 concentration was checked by the on-line gas chromatograph (SP-6890, Rui Hong in South Shandong, China) and recorded every 2 minutes. When the CO_2 concentration in the outlet (C) was equal to that in the inlet (C_0), an adsorption process finished. Subsequently, the feed gas was transferred to N_2 and the temperature was heated up to 100 °C to desorb the adsorbed CO_2. When the value of C was 0, a desorption process ended. Ten adsorption–desorption cycles were performed to study the regenerability of the semicoke-based sorbent.

When $C/C_0 = 0.05$, the breakthrough adsorption stage finished, here the adsorption time and adsorption capacity were named as the breakthrough time and breakthrough adsorption capacity. When $C/C_0 = 1$, the adsorption reached equilibrium or saturation, and the corresponding adsorption capacity was equilibrium adsorption capacity. In general, the breakthrough time and breakthrough adsorption capacity often used to evaluate the adsorption efficiency and kinetics, and the equilibrium adsorption capacity used to evaluate the adsorption capacity. When the adsorption capacity, especially the breakthrough adsorption capacity is over 2 mmol g^{-1}, the sorbent is considered to be of potential application.[35]

2.4. Characterization

The pore structure properties of the activated semicoke before and after HCl washing were characterized by the physical adsorption of N_2 at 77 K using a Quadrasorb SI analyzer (Quantachrome Instruments, United States). The specific surface area was calculated by the Brunauer–Emmett–Teller (BET) equation, and the pore volume was gained on the basis of the adsorption amount of N_2 at a relative pressure of 0.974, then the pore size distribution was identified through the Barrett–Joyner–Halenda (BJH) model from the desorption branch.

To intuitively determine the effect of activation temperature on the pore development of the semicoke, the surface

morphology of the semicoke activated at different temperature were recorded using a JSM-7500F scanning electron microscope (JEOL, Japan) at 5.0 kV.

3. Results and discussions

3.1. Characterization

According to the previous study, the semicoke activated at 700 °C for 2 h suggested a typical crack-type mesoporous and macroporous structure, with mesopores centering at 20–30 nm.[32] Here, the pore structures of the semicoke activated at different temperature are shown in Table 1. Before and after HCl treating, the BET surface area and total pore volume of the activated semicoke all first increased and then decreased with the activation temperature increasing from 600 °C to 800 °C. To the semicoke activated at a same temperature, HCl treating caused the BET surface area and total pore volume increased, suggesting the reaming effect of HCl washing. It is worth noting that before and after HCl washing, the average pore size all increased as the activation temperature increased, which may be caused by a greater degree pyrolysis of semicoke at a higher temperature. The higher the temperature, more organics broke down into small gas molecules, thus originally and newly formed pores were amplified and the average pore size increased. However, excessive activation might cause small pores merging into large pores or partial pores collapsing, so the BET surface area and pore volume didn't continuously increase as the temperature increased.

The scanning electron microscopy (SEM) photographs of the semicoke activated at 600, 700 and 800 °C are shown in Fig. 1.

Table 1 The textural properties of the activated semicoke before and after HCl-treating

Sorbent	BET surface area (m^2 g^{-1})	Total pore volume (cm^3 g^{-1})	Average pore size (nm)
SE600-2	15.2	0.031	33.1
SE700-2	20.5	0.042	49.9
SE800-2	19.9	0.040	52.6
SE600-2(6)	20.3	0.041	38.8
SE700-2(6)	27.1	0.050	51.2
SE800-2(6)	25.5	0.046	54.7

As the temperature increased from 600 to 700 °C, the pores and cracks in the semicoke were more and more developed, causing the BET surface area and pore volume increased. At 800 °C, the larger degree pyrolysis of organics gave rise to already formed pores merging or collapsing, therefore, the pores and cracks were enlarged, which is in accordance with the results of the pore structure data.

3.2. Dynamic CO_2 adsorption performance of the prepared sorbents

3.2.1. Effect of the activation temperature. To investigate the effect of the activation temperature on the adsorption performance of the semicoke, the breakthrough curves and adsorption capacity of the activated semicoke at 20 °C are shown in Fig. 2.

As shown in Fig. 2(a), as the temperature increased from 600 to 900 °C, the breakthrough curve first moved to the right and then to the left, suggesting that the corresponding adsorption performance first increased and then decreased, and the corresponding breakthrough and equilibrium adsorption data are shown in Fig. 2(b). For SE600-2, the equilibrium adsorption capacity was 2.14 mmol g^{-1}, and for SE700-2, the equilibrium adsorption capacity was 2.70 mmol g^{-1}, but for SE900-2, the equilibrium adsorption capacity was dropped to 1.94 mmol g^{-1}. According to the previous FT-IR characterization,[32] in the process of N_2 activation, the peaks of the semicoke at 1020 and 1383 cm^{-1} appeared, which separately representing the asymmetric stretching vibration of C–O–C in the aliphatic ether and aromatic ether. As the activation temperature increased, the pores and cracks became more developed, in which the ether groups became more abundant. As a proton acceptor, more ether groups reacted with CO_2 by dipole interactions, thus the increase of the activation temperature helped CO_2 adsorb in the semicoke. However, excessively high temperature blocked the pores and cracks development, and the CO_2 adsorption performance correspondingly decreased. The activation temperature of 700 °C was a suitable choice.

3.2.2. Effect of HCl-treating and TEPA-functionalizing. HCl-treating could remove the tar coated both in and on the surface of the pores and cracks, and promote the development of pores and cracks. Here, the HCl of 6 mol L^{-1} was used to wash the semicoke activated at different temperature, then

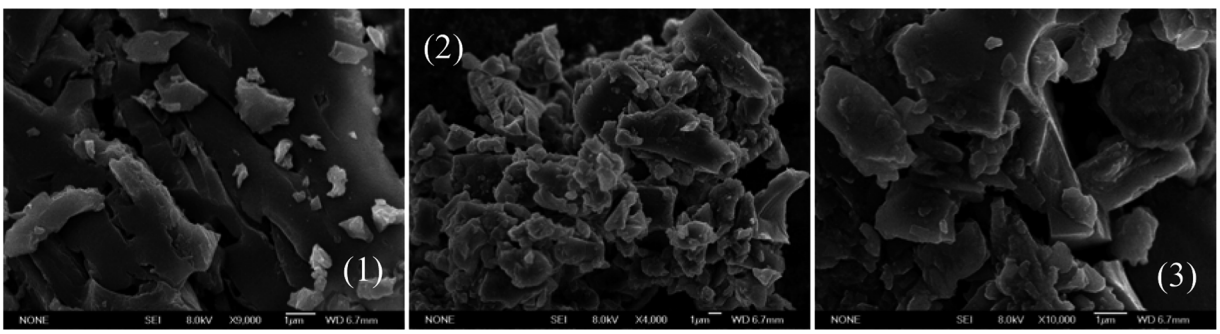

Fig. 1 The SEM photographs of (1) SE600-2, (2) SE700-2 and (3) SE800-2.

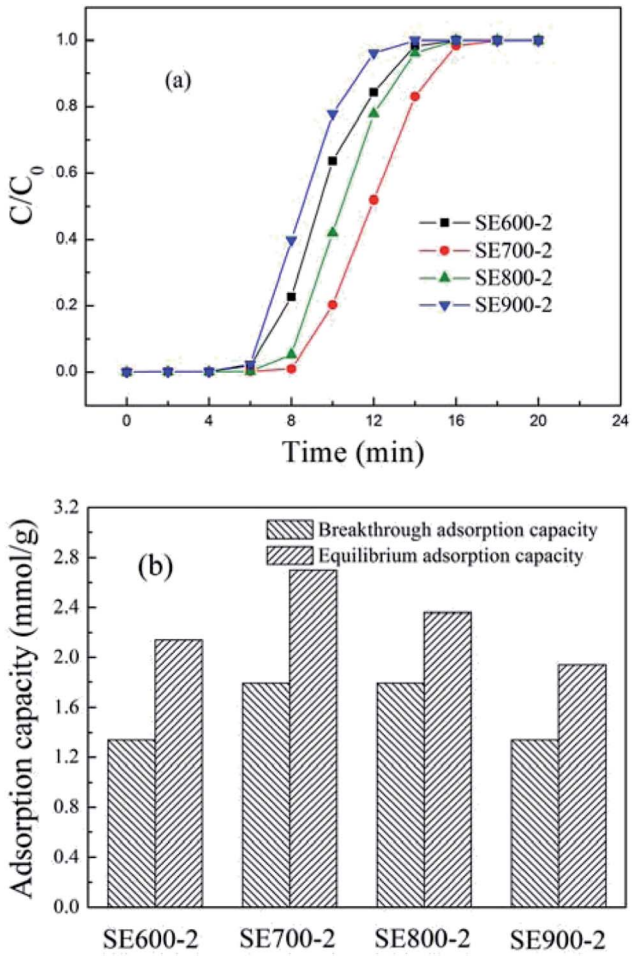

Fig. 2 The breakthrough curves and adsorption capacity (at 20 °C) of the semicoke activated at different temperature.

10 wt% of TEPA was used to further functionalize the activated semicoke before and after HCl-treating.

The CO_2 adsorption experiments of the TEPA-functionalized semicoke before and after HCl treating were performed at 60 °C, and the breakthrough curves and corresponding equilibrium adsorption capacity are shown in Fig. 3. Comparing Fig. 3(a) with Fig. 2(a), the TEPA-functionalization improved the adsorption performance of the activated semicoke, which was mainly due to the introduction of the well-dispersed amine groups in the pores and cracks of the activated semicoke. The amine groups from TEPA interacted with CO_2 not only at a molar ratio of 2 : 1, but also at a ratio of 1 : 1 under the synergistic effect between the ether groups and amine groups,[10] and the reactions are as follows.

$$2R_2NH + CO_2 \rightleftharpoons R_2NH_2^+ + R_2NCOO^- \quad (1)$$

$$RR'O + R_2NH + CO_2 \rightleftharpoons RR'OH^+R_2NCOO^- \quad (2)$$

As seen in Fig. 3(a)–(c), HCl-treating improved the adsorption performance of the TEPA-functionalized semicoke a lot, with the result being similar with the previous study.[32] HCl-

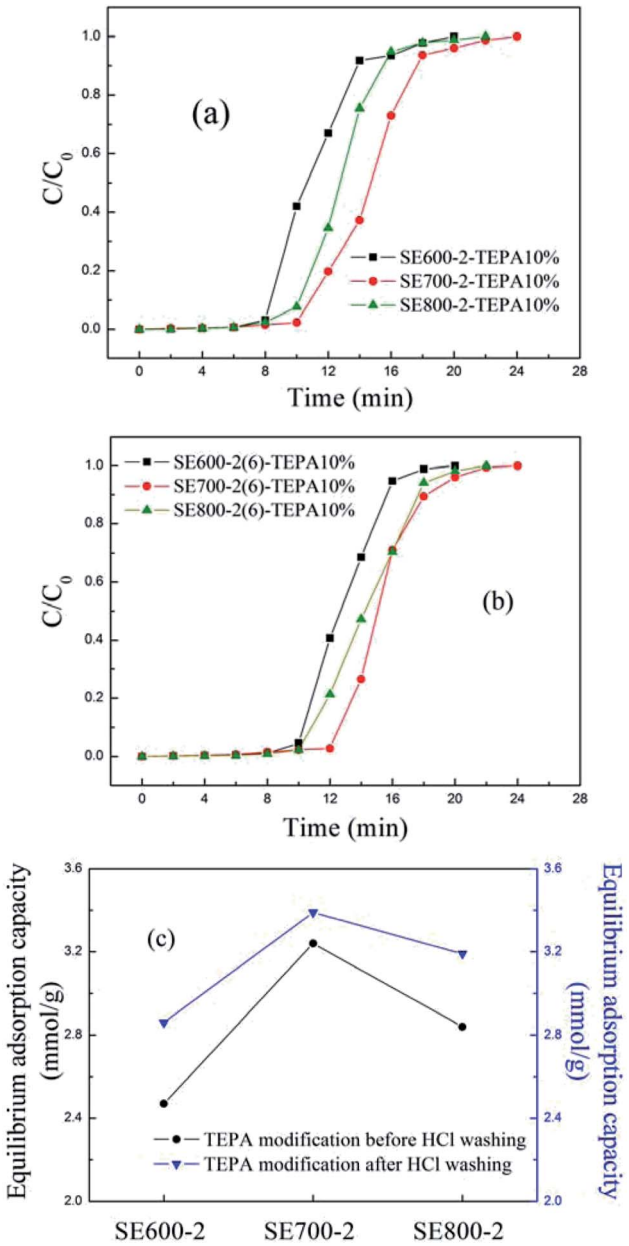

Fig. 3 The breakthrough curves and equilibrium adsorption capacity (at 60 °C) of the TEPA-functionalized activated semicoke before and after HCl-treating.

treating could remove the tar coated both in and on the surface of the pores and cracks, improve the development of pores and cracks, and help more ether groups expose. Therefore, HCl-treating promoted CO_2 adsorb in the activated semicoke. At 60 °C, the breakthrough and equilibrium adsorption capacity for SE700-2(6)-TEPA10% were separately 2.68 and 3.39 mmol g^{-1}, and the sorbent is potentially applicable in capturing CO_2 from flue gases in the coal-fired power plants.

3.2.3. Effect of the activation time. Different activation time caused different decomposition degree of the organics in the semicoke, different development extent of the pores, cracks and surface functional groups, which all have effect on the CO_2 adsorption performance of the activated semicoke. To

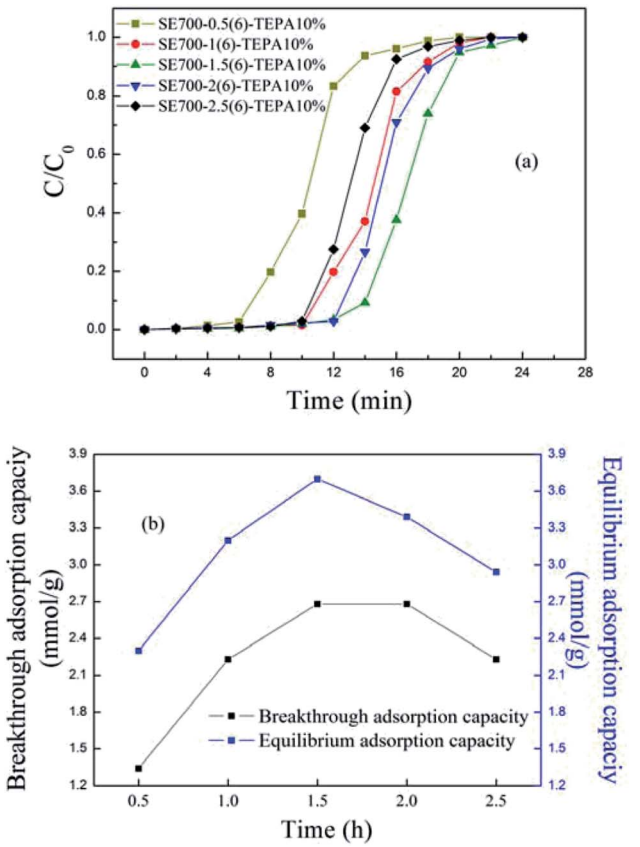

Fig. 4 The (a) breakthrough curves and (b) adsorption capacity of the TEPA-functionalized semicoke activated for different time.

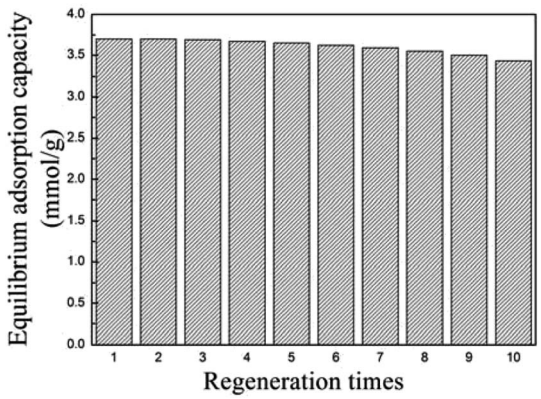

Fig. 5 The equilibrium adsorption performance of SE700-1.5(6)-TEPA10% after ten times of regeneration.

investigate the effect of the activation time, the semicoke activated for different time was first HCl-treated and then TEPA-functionalized to study its CO_2 adsorption performance. Fig. 4 shows the (a) breakthrough curves and (b) adsorption capacity of the semicoke-based sorbents activated for different time.

As shown in Fig. 4(a), the breakthrough curves first moved to the right and then to the left, with the optimal adsorption appearing when the activation time was 1.5 h, and both the breakthrough and equilibrium adsorption suggested the same variation trend as seen from Fig. 4(b). As the activation time increased, the decomposition of organics in the semicoke became more and more adequate, with the pores, cracks and surface functional groups being more and more developed, thus promoting CO_2 adsorb in the semicoke. However, excessive activation might cause pores and cracks collapsing, and weakened the adsorption performance of the semicoke-based sorbents. Therefore, the adsorption performance of the activated semicoke first increased and then decreased as the activation time increased. For SE700-1.5(6)-TEPA10%, the breakthrough and equilibrium adsorption capacity were separately 2.68 and 3.70 mmol g^{-1}, with the rapid and efficient breakthrough stage meeting the requirement of 2–3 mmol g^{-1} in the industry.

3.3. Regenerability of the TEPA-functionalized activated semicoke

Good regenerability is an important index for evaluating a sorbent. Here, the SE700-1.5(6)-TEPA10% with good breakthrough and equilibrium adsorption performance was regenerated for ten times to study its regeneration performance. As seen from Fig. 5, the equilibrium adsorption capacity didn't show obvious change after three adsorption–desorption cycles, and then suggested slightly decrease. After ten regenerations, the equilibrium adsorption capacity was 3.43 mmol g^{-1}, which still accounts for 92.7% of that for the fresh sorbent and has comparable regenerability with that of the TEPA/PEI-modified mesoporous capsules[11] and amine-modified SBA-15,[36] showing the good regenerability of the activated semicoke-based sorbent.

4. Conclusion

The activated semicoke, which is obtained by activating the semicoke from the low-rank lignite, not only has good breakthrough and equilibrium adsorption performance at room temperature, but also has simple and easy preparation process. After HCl-treating, the TEPA-functionalized semicoke activated at 700 °C showed good CO_2 adsorption performance at 60 °C, with the breakthrough and equilibrium adsorption capacity separately reaching 2.68 and 3.70 mmol g^{-1} when the activation time was 1.5 h. The activation process formed abundant ether functional groups, which promoted the synergistic effect among functional groups and helped CO_2 adsorption. In addition, the TEPA-functionalized semicoke-based sorbent suggested efficient breakthrough adsorption stage and good regenerability, and showed potential application in CO_2 capture from flue gases.

Conflicts of interest

There are no conflicts of interest to declare.

Acknowledgements

The financial support from the Natural Science Foundation of Shandong Province (Grant No. ZR2017BEE038), the Foundation

of State Key Laboratory of High-efficiency Utilization of Coal and Green Chemical Engineering (Grant No. 2017-K29) and the Doctoral Research Program of Weifang University (Grant No. 2017BS07) are gratefully acknowledged.

References

1 G. Bala, L. Bopp, V. Brovkin, J. Canadell and A. Chhabra, *Working Group I Contribution to the IPCC Fifth Assessment Report (AR5), Climate Change 2013: The Physical Basis, Working Group I-Twelfth Session*, Intergovernmental Panel on Climate Change (IPCC), Geneva, Switzerland, 2013.

2 D. P. Vargas, M. Balsamo, L. Giraldo, A. Erto, A. Lancia and J. C. Moreno-Pirajan, Equilibrium and dynamic CO_2 adsorption on activated carbon honeycomb monoliths, *Ind. Eng. Chem. Res.*, 2016, **55**, 7898–7905.

3 Q. Wang, J. Luo, Z. Zhong and A. Borgna, CO_2 capture by solid adsorbents and their applications: current status and their new trends, *Energy Environ. Sci.*, 2011, **4**, 42–55.

4 D. P. Vargas, M. Balsamo, L. Giraldo, A. Erto, A. Lancia and J. C. Moreno-Pirajan, Equilibrium and dynamic CO_2 adsorption on activated carbon honeycomb monoliths, *Ind. Eng. Chem. Res.*, 2016, **55**, 7898–7905.

5 X. Wang, L. Chen and Q. Guo, Development of hybrid amine-functionalized MCM-41 sorbents for CO_2 capture, *Chem. Eng. J.*, 2015, **260**, 573–581.

6 E. S. Sanz-Perez, M. Olivares-Marín, A. Arencibia, R. Sanz, G. Calleja and M. M. Maroto-Valer, CO_2 adsorption performance of amino-functionalized SBA-15 under post-combustion conditions, *Int. J. Greenhouse Gas Control*, 2013, **17**, 366–375.

7 X. Wang, Q. Guo, J. Zhao and L. Chen, Mixed amine-modified MCM-41 sorbents for CO_2 capture, *Int. J. Greenhouse Gas Control*, 2015, **37**, 90–98.

8 J. Y. Kim, J. Kim, S. T. Yang and W. S. Ahn, Mesoporous SAPO-34 with amine-grafting for CO_2 capture, *Fuel*, 2013, **108**, 515–520.

9 D. J. Fauth, M. L. Gray and H. W. Pennline, Investigation of porous silica supported mixed-amine sorbents for post-combustion CO_2 capture, *Energy Fuels*, 2012, **26**, 2483–2496.

10 W. Yan, J. Tang, Z. Bian, J. Hu and H. Liu, Carbon dioxide capture by amine-impregnated mesocellular foam-containing template, *Ind. Eng. Chem. Res.*, 2012, **51**, 3653–3662.

11 G. Qi, Y. Wang, L. Estevez, X. Duan, N. Anako, A. A. Park, W. Li, C. W. Jones and E. P. Giannelis, High efficiency nanocomposite sorbents for CO_2 capture based on amine-functionalized mesoporous capsules, *Energy Environ. Sci.*, 2011, **4**, 444–452.

12 A. Heydari-Gorji, Y. Belmabkhout and A. Sayari, Polyethylenimine-impregnated mesoporous silica: effect of amine loading and surface alkyl chains on CO_2 adsorption, *Langmuir*, 2011, **27**, 12411–12416.

13 C. Chen and S. Bhattacharjee, Trimodal nanoporous silica as a support for amine-based CO_2 adsorbents: improvement in adsorption capacity and kinetics, *Appl. Surf. Sci.*, 2017, **396**, 1515–1519.

14 S. M. Rafigh and A. Heydarinasab, Mesoporous chitosan-SiO_2 nanoparticles: synthesis, characterization, and CO_2 adsorption capacity, *ACS Sustainable Chem. Eng.*, 2017, **5**, 10379–10386.

15 Y. G. Ko, H. J. Lee, H. C. Oh and U. S. Choi, Amines immobilized double-walled silica nanotubes for CO_2 capture, *J. Hazard. Mater.*, 2013, **250–251**, 53–60.

16 O. Jing, C. Zheng, W. Gu, Y. Zhang, H. Yang and L. S. Steven, Textural properties determined CO_2 capture of tetraethylenepentamine loaded SiO_2 nanowires from α-sepiolite, *Chem. Eng. J.*, 2018, **337**, 342–350.

17 K. Sim, N. Lee, J. Kim, E. Cho, C. Gunathilake and M. Jaroniec, CO_2 adsorption on amine-functionalized periodic mesoporous benzenesilicas, *ACS Appl. Mater. Interfaces*, 2015, **7**, 6792–6802.

18 J. Yuan, M. Fan, F. Zhang, Y. Xu, H. Tang, C. Huang and H. Zhang, Amine-functionalized poly(ionic liquid) brushes for carbon dioxide adsorption, *Chem. Eng. J.*, 2017, **316**, 903–910.

19 C. Chen, J. Kim, D. W. Park and W. S. Ahn, Ethylenediamine grafting on a zeolite-like metal organic framework (ZMOF) for CO_2 capture, *Mater. Lett.*, 2013, **106**, 344–347.

20 L. Mafra, T. Čendak, S. Schneider, P. V. Wiper, J. Pires, J. R. B. Gomes and M. L. Pinto, Amine functionalized porous silica for CO_2/CH_4 separation by adsorption: which amine and why, *Chem. Eng. J.*, 2018, **336**, 612–621.

21 L. Mafra, T. Čendak, S. Schneider, P. V. Wiper, J. Pires, J. R. B. Gomes and M. L. Pinto, Structure of cemisorbed CO_2 species in amine-functionalized mesoporous silicas studied by solid-state NMR and computer modeling, *J. Am. Chem. Soc.*, 2017, **139**, 389–408.

22 M. A. O. Lourenço, C. Siquet, J. C. Santos, M. Jorge, J. R. B. Gomes and P. Ferreira, Insights into CO_2 and CH_4 adsorption by pristine and aromatic amine-modified periodic mesoporous phenylene-silicas, *J. Phys. Chem. C*, 2016, **120**, 14236–14245.

23 M. A. O. Lourenço, C. Siquet, M. Sardo, L. Mafra, J. Pires, M. Jorge, M. L. Pinto, P. Ferreira and J. R. B. Gomes, Interaction of CO_2 and CH_4 with functionalized periodic mesoporous phenylene-silica: periodic DFT calculations and gas adsorption measurements, *J. Phys. Chem. C*, 2016, **120**, 3863–3875.

24 W. L. Wang, J. Xiao, J. Ding, X. X. Wang and C. S. Song, Development of a new clay supported polyethylenimine composite for carbon dioxide capture, *Appl. Energy*, 2014, **113**, 334–341.

25 L. Stevens, K. Williams, W. Y. Han, T. Drage, C. Snape, J. Wood and J. Wang, Preparation and CO_2 adsorption of diamine modified montmorillonite *via* exfoliation grafting route, *Chem. Eng. J.*, 2013, **215–216**, 699–708.

26 M. Sarmah, B. P. Baruah and P. Khare, A comparison between CO_2 capturing capacities of fly ash based composites of MEA/DMA and DEA/DMA, *Fuel Process. Technol.*, 2013, **106**, 490–497.

27 S. Ottiger, R. Pini, G. Storti and M. Mazzotti, Competitive adsorption equilibria of CO_2 and CH_4 on a dry coal, *Adsorption*, 2008, **14**, 539–556.

28 X. Wang and Q. Guo, CO_2 adsorption behavior of activated coal char modified with tetraethylenepentamine, *Energy Fuels*, 2016, **30**, 3281–3288.
29 L. Brochard, M. Vandamme, J.-M. R. Pellenq and T. Fen-Chong, Adsorption-induced deformation of microporous materials: coal swelling induced by CO_2-CH_4 competitive adsorption, *Langmuir*, 2012, **28**, 2659–2670.
30 G. Gürdal and M. N. Yalçın, Gas adsorption capacity of carboniferous coals in the zonguldak basin (NW turkey) and its controlling factors, *Fuel*, 2000, **79**, 1913–1924.
31 S. Ramasamy, P. P. Sripada, M. M. Khan, S. Tian, J. Trivedi and R. Gupta, Adsorption behavior of CO_2 in coal and coal char, *Energy Fuels*, 2014, **28**, 5241–5251.
32 X. Wang, D. Wang, M. Song, C. Xin and W. Zeng, Tetraethylenepentamine-modified activated semicoke for CO_2 capture from flue gas, *Energy Fuels*, 2017, **31**, 3055–3061.
33 P. L. Younger, Hydrogeological and geomechanical aspects of underground coal gasification and its direct coupling to carbon capture and storage, *Mine Water Environ.*, 2011, **30**, 127–140.
34 C. Laxminarayana and P. J. Crosdale, Role of coal type and rank on methane sorption characteristics of Bowen basin, Australia coals, *Int. J. Coal Geol.*, 1999, **40**, 309–325.
35 X. Wang, Q. Guo and T. Kong, Tetraethylenepentamine-modified MCM-41/silica gel with hierarchical mesoporous structure for CO_2 capture, *Chem. Eng. J.*, 2015, **273**, 472–480.
36 X. Yan, L. Zhang, Y. Zhang, G. Yang and Z. Yan, Amine-modified SBA-15: effect of pore structure on the performance for CO_2 capture, *Ind. Eng. Chem. Res.*, 2011, **50**, 3220–3226.